

# BE/APh 161: Physical Biology of the Cell

Justin Bois

Caltech

Winter, 2016

### 3 Mathematizing cartoons

The word “model” in biology has many meanings. There are three main ones, so far as I can tell.

**Cartoons models.** These models are the typical cartoons or qualitative verbal descriptions we see in text books or in discussion sections of biological papers. They are a sketch of what we think might be happening in a system of interest, but they do not provide quantifiable predictions.

**Physical models.** These models give quantifiable predictions that must be true if a hypothesis (which is often sketched as a *cartoon*) is true. Sometimes hard work and deep thought are needed to generate quantitative predictions. This often requires “mathematizing” the cartoon. This is how a *physical model* is derived from a *cartoon*. Oftentimes when biological physicists refer to a “model,” they are talking about a physical model.

**Statistical models.** A statistical model specifies how we expect measured data to behave using the language of probability. Specifically, it describes how the measurements are expected to vary from the *physical model* because of measurement noise and other sources of variation.

In this class, we will be working mainly on physical models. The connection of these models to their respective cartoons is of paramount importance. We often think of biological systems in terms of the cartoons, and we need to understand what parameters and what quantifiable measurements result from the cartoons. Perhaps most importantly, we need to know what falsifiable hypotheses follow from a cartoon.

In this lecture, we will learn how to go from a cartoon to a physical model. The authors of *PBoC2* call this “mathematizing a cartoon.” We will do this mainly by example, and you will get a chance to practice other examples in the homework throughout the course.

There is a [companion Jupyter notebook to this lecture](#) that has the details of the numerical calculations.

#### 3.1 Flagellar growth and length control in *Chlamydomonas reinhardtii*

We will cut our physical modeling teeth on a beautiful system: the growth of flagella in *Chlamydomonas reinhardtii*. *Chlamydomonas* has two flagella of the same length that it uses to swim. These flagella are constructed from microtubules arranged in a fascinating structure called an *axoneme*. The flagella are thought to be built

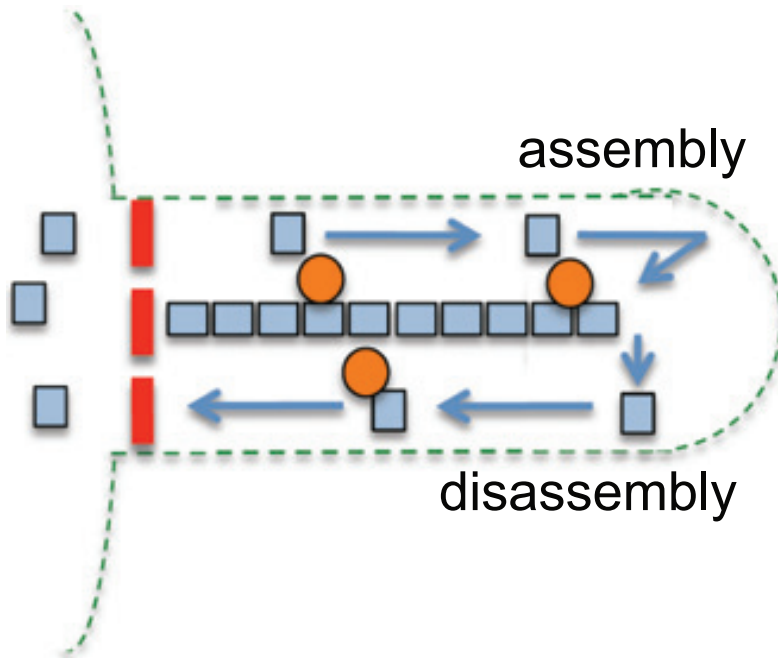


Figure 1: A cartoon sketch of the balance point model. Motor proteins (Orange circles) transport tubulin (blue squares) and other necessary axoneme growth elements to the distal tip of the flagellum. There is spontaneous disassembly at the tip. Figure taken from Avasthi and Marshall, *Differentiation*, 83, S30-S42, 2012.

### 3.1.1 Our first try: a simple model

As a first try at modeling assembly, we assume the motors deliver tubulin to the tip of the flagellum at a constant rate  $\beta$  and that the microtubules depolymerize from the time at a constant rate  $\alpha$ . Then, the length of the flagellum, measured in units of number of added tubulin dimers is described by the differential equation

$$\frac{d\ell}{dt} = \beta - \alpha. \quad (3.1)$$

The solution to this differential equation is

$$\ell(t) = \ell_0 + (\beta - \alpha)t. \quad (3.2)$$

This is obviously not the case, because the flagellum would grow without bound (assuming  $\beta > \alpha$ ). So, by mathematizing the model, we have immediately exposed a certain model as unfeasible.

### 3.1.2 A refinement: the “balance point model”

Marshall and Rosenbaum (2001) proposed a refinement on our first simple model. They noted that there are a constant number of motor proteins present in the flagel-

lum as it grows. So, the density of motors is greater early on in the growth (when it is short) and more sparse later on (when it is long). We might estimate that the rate of delivery of material to the tip of the microtubule is then proportional to the motor density,  $\rho = N_{\text{IFT}}/\ell$ , where  $N_{\text{IFT}}$  is constant. Now, the dynamics read

$$\frac{d\ell}{dt} = \beta/\ell - \alpha, \quad (3.3)$$

where we have wrapped constants into the parameter  $\beta$  such that  $\beta \propto N_{\text{IFT}}$ . Now, we have a steady state length of  $\beta/\alpha$ . Now, let's look at this equation and see what it tells us about microtubule growth.

It is often good practice, especially when doing a numerical solution, to **nondimensionalize** the equations first. This limits the number of parameters we need to vary. For the balance point model, we have two parameters,  $\beta$  and  $\alpha$ , which have units of length squared per time and length per time, respectively. We can then construct characteristic length scale  $\beta/\alpha$  and characteristic time scale  $\beta/\alpha^2$ . We then define dimensionless length  $\tilde{\ell}$  via  $\ell = \beta\tilde{\ell}/\alpha$  and dimensionless time  $\tilde{t}$  via  $t = \beta\tilde{t}/\alpha^2$ . Substituting these expressions into the balance point model gives

$$\frac{d\tilde{\ell}}{d\tilde{t}} = \tilde{\ell}^{-1} - 1. \quad (3.4)$$

Now, let's consider some limits of the differential equation. In the long time limit, as it approaches steady state,  $\tilde{\ell} \rightarrow 1$ . We can expand the right hand side in a Taylor series about  $\tilde{\ell} = 1$  to see how the growth rate approaches the steady state length. To first order in  $\tilde{\ell} - 1$ , we get

$$\frac{d\tilde{\ell}}{d\tilde{t}} = 1 - \tilde{\ell}. \quad (3.5)$$

Thus, as we approach the steady state length,

$$1 - \tilde{\ell} \sim e^{-\tilde{t}}, \quad (3.6)$$

meaning that it approaches the asymptote exponentially.

The short-time limit is not really accessible here, since we cannot take a limit of  $\ell \rightarrow 0$ . Our physical model does not really allow this either, as this implies an infinite density of the IFT particles.

Now, the solution to the differential equation results in either a transcendental equation for  $x$  or use of the Lambert-W function. Either way, the solution is ugly and not terribly informative. I am generally of the opinion that solving differential equations is only useful if the solution provides some insight or enables that taking of some limit. When all we can get is plot the solution, we are equally well-served by solving the differential equation numerically.

### 3.1.3 The balance point model and experiment

Engel, Ludington, and Marshall (Engel, et al., *J. Cell Biol.*, **187**, 81-89, 2009) measured the growth of flagella after pH shock, which eliminates the flagella. I digitized their result from Fig. 1 of that paper and performed a nonlinear regression using the balance point model. The details of the calculation can be found in the [companion Jupyter notebook to this lecture](#). The results are shown in Fig. 2 This provides

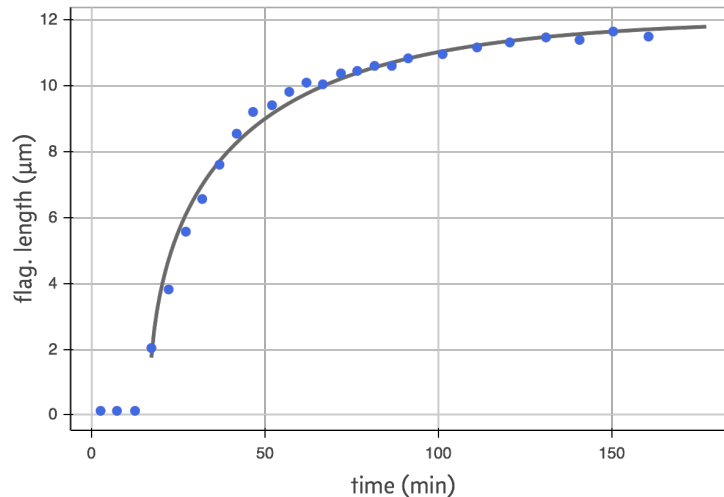


Figure 2: Curve fit of the balance point model to the data digitized from the Engel, et al., paper. The best fit parameters as  $\alpha = 0.23 \mu\text{m}/\text{s}$  and  $\beta = 2.74 \mu\text{m}^2/\text{s}$ .

convincing evidence that the balance point model might be describing microtubule growth dynamics.

### 3.1.4 Testing the balance point model

The balance point model, as we have formulated it, assumes each flagellum is independent of all others. Therefore, if we sever one flagellum and watch it grow back, the other flagellum should be unaffected under the model. Ludington and coworkers devised a clever experiment in which they trapped individual *Chlamydomonas* cells using a microfluidic device and then used a laser to sever one of the flagella (see Fig. 3).

Ludington and coworkers instead saw that the length of the non-severed microtubule shrunk while the other grew, as show in Fig. 4 This means that the two are not independent.

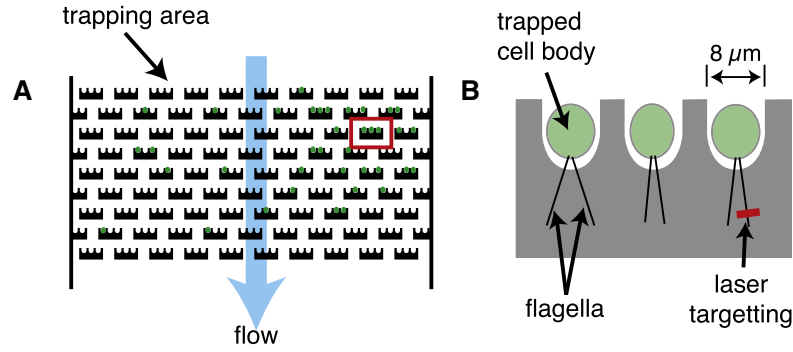


Figure 3: A) Schematic of microfluidic device for trapping of individual *Chlamydomonas* cells. B) Trapped cells and laser ablation setup. Figure take from Ludington, et al., *Curr. Biol.*, **22**, 2173–2179, 2012.

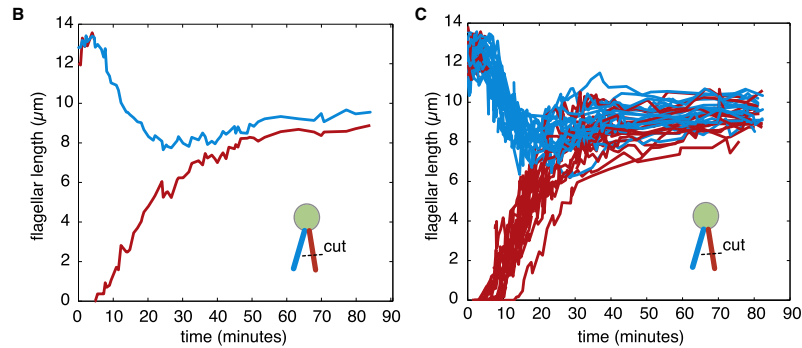


Figure 4: B) Results from a single laser ablation-regrowth experiment. C) The response of 20 cells who had flagella ablated simultaneously in the same microfluidic chamber. Figure taken from Ludington, et al., *Curr. Biol.*, **22**, 2173–2179, 2012.

### 3.1.5 Updating the balance point model

There is clearly some connection between the two flagella. What might this connection be? One hypothesis is that the two flagella share a cytoplasmic pool of tubulin. Specifically, let  $n$  be the number of axoneme components (which we'll just call precursor for brevity) in the cytoplasm available for incorporation into the flagella. We will again use units of  $\mu\text{m}$  for  $n$ . Then the amount of precursor that an IFT train at the base of the flagellum can pick up is a function of  $n$ . This is expressed in the cartoon in Fig. 5

We will now write down an updated balance point model for two flagella that share the same (conserved) cytoplasmic pool of precursor. We use units of concentration that are consistent with flagellar length. That is, concentrations are units of  $\mu\text{m}$  per volume. Let  $l_1$  and  $l_2$  be the lengths of the respective microtubules. Let the anterograde IFT train speed be  $v_a$  and the retrograde IFT train speed by  $v_r$ . The time it takes an IFT train to reach the tip is  $l_i/v_a$ , and the amount of time it takes the disassembled particles to reach the base is  $l_i/v_r$ . We will approximate the rate of pickup

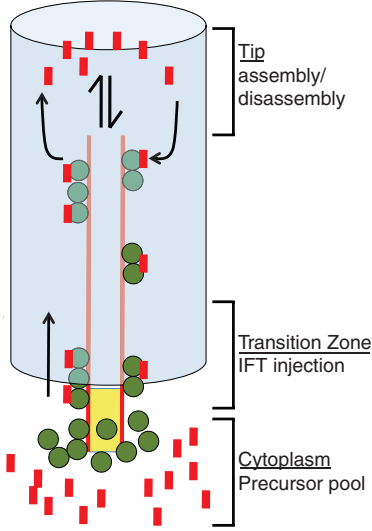


Figure 5: An updated balance point model where the cytoplasm contains a pool of axoneme components to be transported by motor proteins to the tip. Figure taken from Chan and Marshall, *Science*, 337, 1186–1189, 2012.

of precursor at the base as a linear function of the train density and the cytoplasmic concentration. (Remember that the density of transporters goes like  $1/\ell_i$ .) Then, we can write delayed differential equations describing the length of the flagella.

$$\frac{d\ell_1}{dt} = \beta \frac{n(t - \ell_1/v_a)}{\ell_1} - \alpha, \quad (3.7)$$

$$\frac{d\ell_2}{dt} = \beta \frac{n(t - \ell_2/v_a)}{\ell_2} - \alpha. \quad (3.8)$$

We can write a differential equation for removal and delivery from the cytoplasm.

$$\frac{dn}{dt} = -\beta n \left( \frac{1}{\ell_1} + \frac{1}{\ell_2} \right) + 2\alpha. \quad (3.9)$$

Here,  $V$  is the volume in which the precursor particles reside. (This may be the entire, well mixed cell, or so pocket in the cytoplasm where the precursors are localized.) Note that here,  $\beta$  has a different meaning than before. Its units are now  $\mu\text{m}/\text{s}$ . Note also that even though tubulin that is disassembled from the tip takes a time  $\ell_i/v_r$  to return to the cytoplasm, there is no explicit time delay in the  $n$  dynamics because this is a constant process.

We also have conservation of total flagellar material.

$$n_{\text{tot}} = n + \ell_1 + \ell_2. \quad (3.10)$$

These equations allow us to compute the steady state. From the dynamics of  $\ell_1$  and  $\ell_2$ , it is clear that  $\ell_1 = \ell_2 = \beta n/\alpha$  at steady state. Inserting this expression into the

conservation law gives the steady state.

$$n = \frac{\alpha n_{\text{tot}}}{\alpha + 2\beta}. \quad (3.11)$$

### 3.1.6 Nondimensionalization of the updated balance point model

To nondimensionalize, we need to choose units for  $\ell_1$  and  $\ell_2$ , which we'll call  $\ell_0$ , units for time,  $\tau$ , and units for the cytoplasmic number of precursors,  $n_0$ . We define  $\ell_1 = \ell_0 \tilde{\ell}_1$ ,  $\ell_2 = \ell_0 \tilde{\ell}_2$ ,  $t = \tau \tilde{t}$ , and  $n = n_0 \tilde{n}$ . Then, the dynamical equations are

$$\frac{d\tilde{\ell}_1}{d\tilde{t}} = \frac{\beta n_0 \tau}{\ell_0^2} \frac{\tilde{n} \left( \tilde{t} - \frac{\ell_0}{\tau v_a} \tilde{\ell}_1 \right)}{\tilde{\ell}_1} - \frac{\alpha \tau}{\ell_0}, \quad (3.12)$$

$$\frac{d\tilde{\ell}_2}{d\tilde{t}} = \frac{\beta n_0 \tau}{\ell_0^2} \frac{\tilde{n} \left( \tilde{t} - \frac{\ell_0}{\tau v_a} \tilde{\ell}_2 \right)}{\tilde{\ell}_2} - \frac{\alpha \tau}{\ell_0}, \quad (3.13)$$

$$\frac{d\tilde{n}}{d\tilde{t}} = -\frac{\beta \tau}{\ell_0} \tilde{n}(\tilde{t}) \left( \frac{1}{\tilde{\ell}_1} + \frac{1}{\tilde{\ell}_2} \right) + \frac{2\alpha \tau}{n_0}. \quad (3.14)$$

To eliminate parameters, we choose  $\tau = \ell_0/\alpha$  and  $\ell_0/n_0 = \beta/\alpha \equiv \gamma$ . The dimensionless equations then become

$$\frac{d\tilde{\ell}_1}{d\tilde{t}} = \frac{\tilde{n}(\tilde{t} - \tilde{\ell}_1/u)}{\tilde{\ell}_1} - 1, \quad (3.15)$$

$$\frac{d\tilde{\ell}_2}{d\tilde{t}} = \frac{\tilde{n}(\tilde{t} - \tilde{\ell}_2/u)}{\tilde{\ell}_2} - 1, \quad (3.16)$$

$$\frac{1}{\gamma} \frac{d\tilde{n}}{d\tilde{t}} = -\tilde{n}(\tilde{t}) \left( \frac{1}{\tilde{\ell}_1} + \frac{1}{\tilde{\ell}_2} \right) + 2, \quad (3.17)$$

where we have defined  $u \equiv v_a/\alpha$ . We see that the dynamical equations depend only on two parameters: the ratio of pick-up rate of precursor to shedding rate from the tip and the ratio of transport to the tip and shedding rate. To connect to real units, we have to specify one of  $\ell_0$ ,  $n_0$ , or  $\tau$  in terms of  $\alpha$ ,  $\beta$ ,  $n_{\text{tot}}$ , and  $v_a$ , the physical parameters of the system. We could specify  $n_0 = n_{\text{tot}}$ , giving  $\ell_0 = \gamma n_{\text{tot}}$  and  $\tau = \beta n_{\text{tot}}/\alpha^2$ . We note that we always have to make sure that we set initial conditions such that  $\tilde{n} + \gamma(\tilde{\ell}_1 + \tilde{\ell}_2) < 1$  to obey conservation of mass. Any difference of this sum from unity is indicative of precursor material that is in transit in the flagellum, so this sum should be close to unity.



### 3.1.7 Adjusted balance point model and experiments.

We can again fit the adjusted balance point model to growth data from the pH shock experiment. The result is shown in Fig. 6. We again have good agreement with the growth curve.

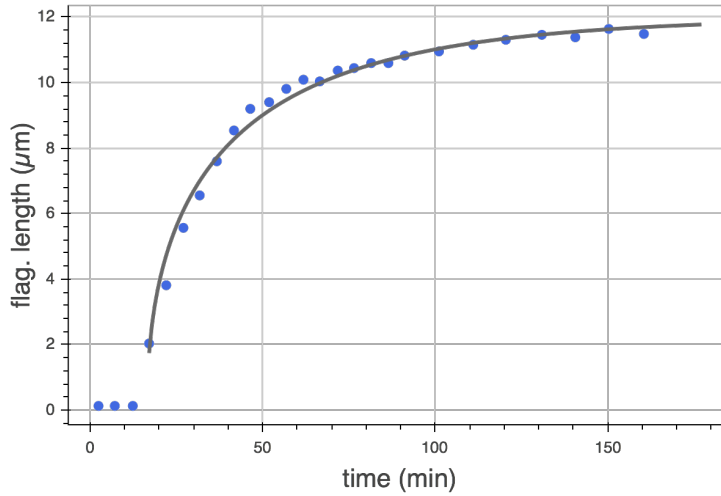


Figure 6: Fit of growth from the pH shock experiment using the adjusted balance point model. The best fit parameters are  $\alpha = 0.073 \mu\text{m}/\text{min}$ ,  $\beta = 0.083 \mu\text{m}/\text{min}$ ,  $n_{\text{tot}} = 37.63 \mu\text{m}$ , and  $\ell_1^0 = \ell_2^0 = 1.74 \mu\text{m}$ .

We now will use these parameters to inform a severing experiment. We start with one filament being the steady state length from the pH shock experiment. We assume that the material that was in the severed flagellum is gone, so that the only precursor available is that which was in the non-severed flagellum and in the cytoplasm. We then numerically solve for the dynamics. The result is shown in Fig. 7. We see the main feature of shrinkage of the intact microtubule while the severed one grows is captured in this model. However, the time scale is too long. This is possibly due to that fact that the parameters were obtained from fitting the pH shock experiment, which has different conditions. We also do not capture the regrowth of the two flagella together that was observed in the experiment. This implies that the cell is making more precursor, which we may want to include in a refinement. This also raises the question of how the cell senses and controls the total amount of tubulin it produces.

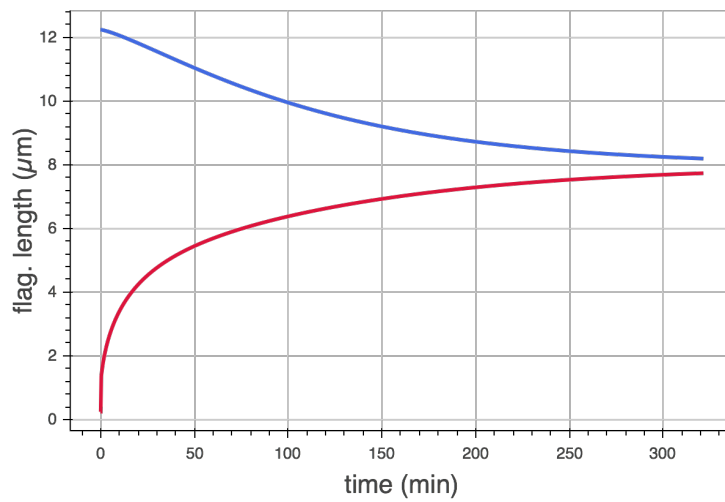


Figure 7: Numerical calculation of severing experiment. The red line shows the length of the severed flagellum and the blue the intact flagellum.